DOI 10.1007/s10946-024-10212-7
Journal of Russian Laser Research, Volume 45, Number 3, May, 2024

AN APPROACH TO DIRECT 3D IMAGING WITH COHERENT LIGHT

I. A. Artyukov, A. S. Busarov, N. L. Popov, and A. V. Vinogradov*

Lebedev Physical Institute, Russian Academy of Sciences
Leninskii Prospect 53, Moscow 119991, Russia

*Corresponding author e-mail: vinograd688@mail.ru

Abstract

We consider the 3D coefficient inverse problem for parabolic wave equation. It involves determining the spatial distribution of refractive and absorption indices by processing phase diffraction patterns obtained by irradiating an object with a set of Gaussian beams. Unlike tomography and ptychography, rotation or scanning of the sample is not required. The problem is solved by expanding the wave field and the complex dielectric constant $\varepsilon(\vec{r})$ over the full set of Gaussian beam functions. To determine $\varepsilon(\vec{r})$, we obtain a nonlinear matrix equation. The condition of its solvability allows the selection of sampling frequencies by coordinates in accordance with the practical task.

Keywords: coherent 3D imaging, coherent diffraction imaging, lens-free 3D imaging, parabolic wave equation, Gaussian beam expansion, time-dependent Schrödinger equation.

1. Initial Equations. Direct Problem

We consider the problem of 3D imaging of amplitude–phase objects. It consists in finding the spatial distribution of the complex dielectric constant $\varepsilon(x, z)$ from the diffraction patterns, which arise when a coherent beam penetrates through an object. The equation for the beam field $u(x, z)$ in the parabolic approximation has the following form [1]:

$$2ik\frac{\partial u(x,z)}{\partial z} + \frac{\partial^2 u(x,z)}{\partial x^2} + k^2[\varepsilon(x,z) - 1]u(x,z) = 0, \qquad u(x,0) = u_0(x), \tag{1}$$

where z is the longitudinal coordinate, k is the wave number, and $u_0(x)$ is the transverse distribution of the incident beam at the input aperture. Equation (1) corresponds to the case of two dimensions. In the case of real 3D space, the other transverse coordinate is added.

For convenience of calculations, we rewrite (1) in the form of the Schrödinger equation as follows:

$$ik\frac{\partial u}{\partial z} = -\frac{1}{2}\frac{\partial^2 u}{\partial x^2} - \frac{k^2}{2}(\varepsilon - 1)u, \qquad u(x,0) = u_0(x) \tag{2}$$

and introduce the notation commonly used in quantum mechanics [2],

$$ik\frac{\partial u(x,z)}{\partial z} = [H_0(x) + V(x,z)]u(x,z), \qquad H_0(x) = -\frac{1}{2}\frac{\partial^2}{\partial x^2} + V_0(x), \qquad V(x,z) = -\frac{k^2}{2}[\varepsilon(x,z) - 1], \tag{3}$$

where, in the general case, $H_0(x)$ is the unperturbed Hamiltonian of the system, and $V(x, z)$ is a perturbation depending on the transverse x and longitudinal z coordinates (analogue of time $t = \mu z/\hbar k$ in

Manuscript submitted by the authors in English on April 11, 2024.

quantum mechanics, with μ being the mass of the particle). If we consider Eqs. (2) and (3) as Schrödinger equations, then the dimension of the coordinate space in them is obviously smaller than in the parabolic equation (1).

The solution to Eq. (3) can be found by expanding $u(x,z)$ in terms of eigenfunctions of the unperturbed Hamiltonian $H_0(x)$ [2,3] or the perturbed Hamiltonian $[H_0(x)+V(x,z)]$ for a fixed z [3,4]. However, in Eq. (2), the potential part of the unperturbed Hamiltonian is equal to zero, $V_0(x)=0$, and Eq. (3) is simplified and reads

$$ik\frac{\partial u(x,z)}{\partial z} = -\frac{1}{2}\frac{\partial^2 u(x,z)}{\partial x^2} + V(x,z)u(x,z), \qquad V(x,z) = -\frac{k^2}{2}[\varepsilon(x,z)-1]. \tag{4}$$

In order to use this equation and satisfy the initial condition in (2), an expansion of $u(x,z)$ over the complete set of solutions $\varphi_m(x,z)$ of the parabolic wave equation in free space suggests itself; see, for example, [5], that

$$u(x,z) = \sum_m c_m(z)\varphi_m(x,z), \tag{5}$$

where

$$ik\frac{\partial \varphi_m(x,z)}{\partial z} = -\frac{1}{2}\frac{\partial^2 \varphi_m(x,z)}{\partial x^2}, \qquad \int \varphi_m^*(x,z)\varphi_n(x,z)dx = \delta_{m,n}; \qquad m,n = 1,2,3\ldots \tag{6}$$

The Hermite–Gauss function, Laguerre–Gauss function, etc. have the properties (6) [6–8]. At the same time, it should be noted that, in numerical calculations, we are certainly limited by the number of terms in the expansion (5), say $m \leq M$.

Substituting (5) into (2) and taking into account (6), we obtain a following system of ordinary differential equations:

$$ik\dot{c}_m(z) = \sum_n V_{mn}(z)c_n(z), \qquad V_{mn}(z) = \int \varphi_m^*(x,z)V(x,z)\varphi_n(x,z)\ dx, \tag{7}$$

$$c_m(0) = \int \varphi_m^*(x,0)u_0(x)\ dx. \tag{8}$$

If to manage formally, we arrive at the equations of nonstationary perturbation theory for a quantum system with degenerate levels. For the purposes of this work, however, the system of equations (7) and (8) seems more convenient than the usual equations of quantum-mechanical perturbation theory, since it does not require to find eigenvalues and eigenfunctions of the unperturbed Hamiltonian. Instead, it is based on well-known special functions, and there are no rapidly oscillating terms, which appear in the standard perturbation theory in matrix elements corresponding to the transitions with changes in energy.

Thus, returning to the beginning of the section, we can say that, in the language of mathematics, the problem of 3D imaging of amplitude–phase objects corresponds to two types of coefficient inverse problems [9]. In one case, we are talking about finding the dielectric constant $\varepsilon(x,z)$ (where x is a set of transverse coordinates) in a three-dimensional parabolic wave equation and, in the others, we are talking about finding the time-dependent potential $V(x,z)$, where the longitudinal coordinate z plays the role of time in the two-dimensional Schrödinger equation.

2. The Inverse Problem and Its Discretization

Equations (7) can serve as a basis for 3D studies of weakly inhomogeneous objects. In this case, we are talking about determining the spatial distribution of the refractive index $n(x,z) = \sqrt{\varepsilon(x,z)}$ of the material. We assume that the object is finite, that is, the optical density $[n(x,z)-1]$ outside the object is zero, and to determine it, the object is illuminated (probed) by coherent beams with a known transverse distribution; the wave field of the transmitted beam is recorded by a detector located in the plane $z = Z$; see Fig. 1.

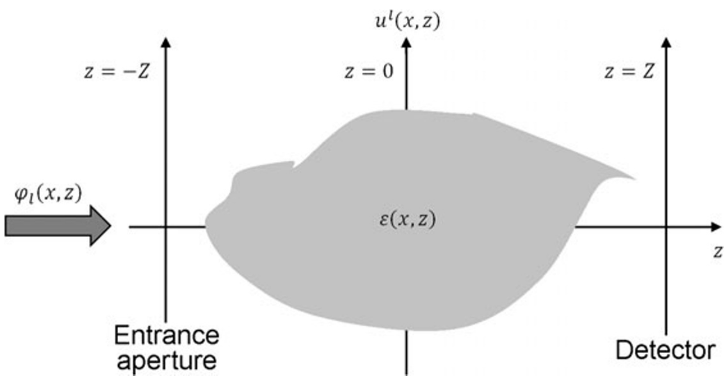

Fig. 1. 3D image of an amplitude–phase object located between the input aperture $(-Z)$ and the detector (Z); here, $u(x,z)$ is the wave field satisfying Eq. (1), and $\varepsilon(x,z)$ is the complex dielectric constant.

As is known, for a flat vertically-located object, for example, in the plane $z = 0$, the problem is solved due to the fact that the field distributions on the object surface and the detector surface are connected by direct and inverse Fourier or Fresnel transforms. This is the basis for experimental 2D "lens-free" methods. The corresponding theoretical approaches are known as the inverse problem of optics [10, 11], coherent diffraction imaging (CDI), phase contrast, ptychography,* and other quantitative microscopy techniques. Extending these techniques to 3D objects is essential for many applications [12–15]. Before doing this, we consider an auxiliary direct scattering problem.

Let a probe beam from the same complete set as in Eqs. (4)–(7) pass through the object under study and try to relate the detector readings to the potential distribution. Taking into account that the object is finite, we have

$$u^l(x,z) = \varphi_l(x,z) \qquad \text{at} \qquad -\infty \le z \le -Z; \qquad l = 1, 2, \ldots L, \tag{9}$$

where $(-Z)$ is the position of the input aperture in front of the left boundary of the object; see Fig. 1, and L is the number of probing beams. At $z \ge -Z$, due to diffraction, the field $u^l(x,z)$ differs from the free space mode $\varphi_l(x,z)$ and satisfies the equation

$$ik\frac{\partial u^l(x,z)}{\partial z} = \left[-\frac{1}{2}\frac{\partial^2}{\partial x^2} + V(x,z)\right] u^l(x,z), \qquad -Z < z < Z. \tag{10}$$

For each of the l probing beams, the reasoning that led to Eqs. (5)–(7) is valid. In particular, the field

*Ptychography is a method to reconstruct the crystal structure (image) of a specimen from the diffraction patterns obtained from each point (area) scanned over a specimen, using a convergent probe so that a part of the illuminated area overlaps. "Ptycho" means "fold" in Greek. This method has been used in X-ray crystal structural analysis; `www.jeol.com/words/emterms/20190212.102107.php` at the receiver $u^l(x,z)$, being similarly to (5), reads

$$u^l(x,Z) = \sum_m c^l_m(z)\varphi_m(x,z)|_{z=Z}, \tag{11}$$

where $c^l_m(z)$ are the expansion coefficients of the field $u^l(x,z)$ over the complete set $\varphi_m(x,z)$. In quantum language, $c^l_m(z=Z)$ are the elements of the scattering matrix, that is, the amplitudes of the probabilities of transitions occurred under the action of perturbation $V(x,z)$. For each l, we obtain a system of ordinary differential equations as follows:

$$ik\dot{c}^l_m(z) = \sum_n V_{mn}(z)c^l_n(z), \tag{12}$$

$$V_{mn}(z) = \int \varphi^*_m(x,z)V(x,z)\varphi_n(x,z)\ dx. \tag{13}$$

From this, one can see that the square matrix $V_{mn}(z)$ describes the propagation of each of the l beams. If we use for probing the entire set of beams $\varphi_m(x,z)$ taken into account in the decomposition (5), that is, $L = M$, then the system of equations (11) is equivalent (in the limit $M \to \infty$) to a following linear differential equation:[†]

$$\frac{d\hat{C}(z)}{dz} = -\frac{i}{k}\hat{V}(z)\hat{C}(z), \qquad \hat{C}(z=-Z) = \hat{I}. \tag{14}$$

For square matrices,

$$\hat{C}(z) = c_{mn}(z) \qquad \text{and} \qquad \hat{V}(z) = V_{mn}(z), \tag{15}$$

where $\hat{I}$ is the unit matrix. If we limit ourselves to a finite number of terms M in Eqs. (11)–(15), the matrices in (14) and (15) also become of the order of M. Then Eq. (14) has a unique solution; see [16].

In the case of a piecewise continuous potential matrix $\hat{V}(z)$, Eq. (14) provides an explicit solution relating the elements of the matrix $\hat{V}(z)$ at the nodes z_s; $s = 1, 2, \ldots, S$, to the output field $u^l(x,z)$ for all l from 1 to M. However, this solution is not sufficient to solve the coefficient inverse problem we are interested in.

To verify this, we assume that the origin of the coordinate system is located at the center of the object; see Fig. 1; this means that

$$V(x,z) = 0 \qquad \text{at} \qquad |z| \geq Z. \tag{16}$$

Next, a piecewise continuous potential in Eq. (14) can be written as

$$\hat{V}(z) = \hat{V}(z_s); \qquad z_{s-1} < z < z_s, \qquad s = 1, 2, \ldots, S = 2Z/h, \tag{17}$$

$$z_s = -Z + s \cdot h; \qquad z_0 = -Z, \ldots, z_S = Z, \tag{18}$$

where S is the number of nodes, and h is the sampling step. Then, the solution to Eq. (14) can be written as a product of matrices [16]; it reads

$$\hat{C}(Z) = \exp\left\{-\frac{ih}{k}\hat{V}(Z)\right\} \cdot \exp\left\{-\frac{ih}{k}\hat{V}(Z-h)\right\} \cdot \ldots \cdot \exp\left\{-\frac{ih}{k}\hat{V}(-Z+h)\right\}\hat{C}(-Z) \tag{19}$$

[†]This is easy to understand by dropping the index l in (11) down to the right.

or, in short, taking into account that $\hat{C}(-Z) = \hat{I}$, we arrive at

$$\hat{C}(Z) = \prod_{1 \le s \le S} \exp\left\{-\frac{ih}{k}\hat{V}(z_s)\right\}. \tag{20}$$

If the matrix $\hat{C}(Z)$ is known, it provides $M \times M$ equations connecting the elements of the perturbation matrices $\hat{V}(z_s)$ with the input and output fields. It is important to note that, in (19) and (20), the order of the multipliers must be observed, as the matrices $\hat{V}(z_s)$ do not commute for different s. In the next section, we explore the possibility of using these equations to solve the coefficient inverse problem, which was formulated in Sec. 1.

3. The Coherent Direct 3D Imaging Equation and Solvability Condition

Thus, following Sec. 2, we assume that an object, represented by a piecewise continuous perturbation, $\hat{V}(Z)$, is probed by Gaussian beams. Then the matrix $\hat{C}(Z)$, which, according to Eqs. (15) and (13), defines the field at the detector located behind the object, has the following form:

$$\hat{C}(Z) = \prod_{1 \le s \le S} \exp\left\{-\frac{ih}{k}\hat{V}(z_s)\right\}. \tag{21}$$

The field at the detector arising at the incidence of a Gaussian beam is a superposition of Gaussian beams; it reads

$$u^l(x, Z) = \sum_m c_{ml}(Z)\varphi_m(x, Z). \tag{22}$$

By entering the pixel coordinates x_p of the detector, $p = 1, 2 \ldots P$, we obtain a system of nonlinear equations to determine the elements of the perturbation matrices $V_{mn}(z_s)$, namely,

$$u^l(x_p, Z) = \sum_m c_{ml}(Z)\varphi_m(x_p, Z), \tag{23}$$

where $u^l(x_p, Z)$ is the set of detector readings, and $\varphi_m(x_p, Z)$ are the values of the Gaussian functions in the detector plane.

Here, it should be emphasized that the detector, in this work, is assumed to be a phase detector; more precisely, it allows to measure both the amplitude and phase of the electromagnetic field. This is possible in the terahertz and longer wavelength ranges. At shorter wavelengths, the detectors are quadratic, i.e., they record the intensity or energy density of the field. Therefore, since the 1970s, special numerical methods (phase retrieval) for processing images and diffractograms of non-crystalline objects have been developed to restore the phase. They are widely used, especially in the case of coherent radiation sources [12].

To determine $c_{ml}(Z)$, in view of (23), a full number of pixels, $P = M$, is required. Once $c_{ml}(Z)$ are found, the desired elements of the perturbation matrices, $V_{mn}(z_s)$, must be determined, using the relations

$$c_{ml}(Z) = \left\{\prod_{1 \le s \le S} \exp\left[-\frac{ih}{k}\hat{V}(z_s)\right]\right\}_{ml}, \tag{24}$$

which follow from (21). Thus, Eqs. (23) and (24) seem to basically solve the problem of volumetric visualization of amplitude–phase objects.

However, let us take a closer look at Eqs. (24); these are M^2 equations with SM^2 unknown variables, and they can only be solved for $S = 1$, i.e., only for one plane. This is of a little practical interest. You can change this situation by expanding the perturbation (dielectric constant) into a series, for example, using Gaussian functions,

$$V(x,z) = \sum_j W_j(z)\varphi_j(x,z); \qquad j = 1,\ldots,J \qquad \text{where} \qquad W_j(z) = \int \varphi_j^*(x,z)V(x,z)\,dx. \tag{25}$$

Substituting $V(x,z)$ from (25) into (7), one obtains

$$V_{m,n}(z) = \sum_j W_j(z)\cdot B^j_{mn}(z), \qquad B^j_{mn}(z) = \int \varphi_m^*(x,z)\varphi_j(x,z)\varphi_n(x,z)\,dx. \tag{26}$$

Thus, in view of (25), it is possible to describe the perturbation $V(x,z)$ in the layer, using J parameters instead of M^2; see (24). This provides flexibility, allowing us to increase the number of layers under study and complete the task. Taking into account (25) and (26), we can derive from (23) and (24) the basic equation for coherent direct 3D imaging; they read

$$u^l(x_p,Z) = \sum_m^M \left[\prod_{1\le s\le S} \exp\left\{-\frac{ih}{k}\sum_{j=1}^J W_j(z_s)\hat{B}^j(z_s)\right\}\right]_{ml} \varphi_m(x_p,Z); \qquad l = 1,\ldots,M. \tag{27}$$

Here, $u^l(x_p,Z)$ is the reading of the pth pixel of the detector, and $W_j(z_s)$ are the coefficients of the potential expansion in Gaussian functions; see (26). Also, $\hat{B}^j(z_s)$ is a matrix composed of products of three Gaussian functions integrated over transverse coordinate x; see (26).

For the purposes of this work, the detector readings $u^l(x_p,Z)$ in Eq. (26) are the input data. The desired values to be found are the expansion coefficients $W_j(z_s)$. The potential $V(x,z)$ (and hence the dielectric constant $\varepsilon(x,z)$ too) can be expressed through these coefficients, in view of formula (25), which, in principle, solves the coefficient inverse problem posed in Sec. 1. The solvability condition for Eqs. (27) is given by

$$P = M = \sqrt{SJ}; \tag{28}$$

it expresses the equality between the number of unknown variables and the number of equations.

4. Discussion and Conclusions

The practical implementation of the proposed approach, which includes the development of computational algorithms and methods for recovering the phase of images, expands the capabilities for studying the internal structure of objects compared to standard computed tomography. First, the material of an object is characterized not only by its absorption index but also by its refractive index. This means that we can obtain more detailed information on the composition and structure of the object. Second, the diffraction problem of electromagnetic radiation passing through an object is solved, using the parabolic equation, rather than the beam approach used in traditional tomography. This allows for a more accurate description of the material properties and morphology.

It should be noted that, in this method, coherent radiation is necessary for probing, but there is no need for rotating the object, detector, or radiation source, as is the case in conventional tomography. Obvious examples of the application of the proposed method are laser physics and coherent microscopy in the visible range, where Gaussian beams are often used as a research tool. Additionally, the technique can be useful in quantum chemistry and nuclear physics, while studying interatomic and internuclear interactions. To solve the inverse problem, in this case, it seems necessary to rely on experimental data on elastic scattering.

In conclusion, we write the equation of the coherent 3D imaging (27) in compact matrix form. To do this, we introduce column vectors describing the wave field in the presence of an object and in a vacuum as follows:

$$U(x,z) = \{u^l(x,z)\}, \qquad l = 1 \ldots L = M \qquad \text{and} \qquad \varphi(x,z) = \{\varphi_m(x,z)\}, \qquad m = 1 \ldots M = L. \tag{29}$$

Then Eq. (27) looks like the following one:

$$u(x_p, Z) = \prod_{1 \le s \le S} \exp\left\{ -\frac{ih}{k} \sum_{j=1}^{J} W_j(z_s) \hat{B}(z_s) \right\} \varphi(x_p, Z). \tag{30}$$

Recall that $\hat{B}(z_s)$ is the square $M \times M$ matrix (26) composed of the integrals from products of three Gaussian functions, $u(x_p, Z)$ is the set of readings of detector, $\varphi(x_p, Z)$ are M sets of values of Gaussian functions at points corresponding to the position of the detector pixels. From these equations, it is necessary to find the coefficients $W_j(z_s)$ that describe according to (26) the 3D-potential (complex dielectric constant).

For the solvability of Eqs. (30), it is necessary to satisfy the following relations:

$$P = M \qquad \text{and} \qquad PM = SJ. \tag{31}$$

They follow from the derivation of the equations for the scattering matrix and its discretization carried out in Secs. 2 and 3. The solvability condition can also be written in a single formula

$$P = M \approx \sqrt{SJ}, \tag{32}$$

where we use approximate equality since fractional numbering can appear here.

Acknowledgments

The authors would like to thank Prof. V. S. Lisitsa, Prof. V. I. Man'ko, Prof. Yu. A. Uspensky, and Prof. I. A. Shchelokov for their discussions.

References

1. M. Levy, *Parabolic Equation Methods for Electromagnetic Wave Propagation*, IET (2000).
2. L. D. Landau and E. M. Lifshitz, *Quantum Mechanics: Non-Relativistic Theory*, Elsevier, Amsterdam (2013), Vol. 3, §40.
3. N. F. Mott and H. S. W. Massey, *Theory of Atomic Collisions*, 3rd ed., Oxford Univ. Press (1965).

4. M. Born and V. Fock, *Zeitschrift für Physik*, **51**, 165 (1928).
5. E. Kieri, G. Kreiss, and O. Runborg, *Adv. Appl. Math. Mech.*, **7**, 687 (2015).
6. E. Abramochkin and V. Volostnikov, *J. Opt. A: Pure Appl. Opt.*, **6**, S157 (2004).
7. H. M. Moya-Cessa, I. Ramos-Prieto, D. Sánchez-de-la-Llave, et al., "Cauchy–Riemann beams," arXiv: 2311.07825 (2023).
8. F. Wu, Y. Luo, and Z. Cui, *Photonics*, **10**, 1041 (2023).
9. A. V. Goncharskii and S. Yu. Romanov, *Comput. Math. Math. Phys.*, **52**, 245 (2012).
10. T. I. Kuznetsova, *Sov. Phys. Usp.*, **31**, 364 (1988).
11. T. S. Argunova and V. G. Kohn, *Physics-Uspekhi*, **62**, 602 (2019).
12. J. Rodenburg and A. Maiden, *Ptychography, Springer Handbook of Microscopy*, Springer Nature Switzerland AG (2019), p. 819.
13. T. Latychevskaia, *Phys. Rev. Lett.*, **127**, 063601 (2021).
14. C. Jacobsen, *X-Ray Microscopy*, Cambridge University Press (2019).
15. Z. Hu, Y. Zhang, P. Li, et al., *Opt. Express*, **31**, 15791 (2023).
16. R. Bellman, *Introduction to Matrix Analysis*, Mcgraw-Hill, New York (1960), Ch. 10, §5.